

# Accepted Manuscript

Obestatin downregulating aquaporin 2 plasma membrane distribution through a short-term regulatory effect

Ming Shen MD , Li-Zhi Bao MD , Xing Zheng MD, PHD ,  
Xian-Xian Zhao MD, PHD , Zhi-Fu Guo MD, PHD

PII: S0002-9629(18)30486-5  
DOI: <https://doi.org/10.1016/j.amjms.2018.12.010>  
Reference: AMJMS 789



To appear in: *The American Journal of the Medical Sciences*

Received date: 1 May 2018  
Accepted date: 22 December 2018

Please cite this article as: Ming Shen MD , Li-Zhi Bao MD , Xing Zheng MD, PHD , Xian-Xian Zhao MD, PHD , Zhi-Fu Guo MD, PHD , Obestatin downregulating aquaporin 2 plasma membrane distribution through a short-term regulatory effect, *The American Journal of the Medical Sciences* (2018), doi: <https://doi.org/10.1016/j.amjms.2018.12.010>

This is a PDF file of an unedited manuscript that has been accepted for publication. As a service to our customers we are providing this early version of the manuscript. The manuscript will undergo copyediting, typesetting, and review of the resulting proof before it is published in its final form. Please note that during the production process errors may be discovered which could affect the content, and all legal disclaimers that apply to the journal pertain.

Obestatin downregulating aquaporin 2 plasma membrane distribution through a  
short-term regulatory effect

Ming Shen, MD, Li-Zhi Bao, MD, Xing Zheng, MD, PHD, Xian-Xian Zhao, MD, PHD, Zhi-Fu Guo,  
MD, PHD

Department of Cardiovascular Diseases, Changhai Hospital, Second Military Medical University,  
Shanghai 200433, China

Corresponding authors: Xian-Xian Zhao, Department of Cardiovascular Diseases, Changhai  
Hospital, Second Military Medical University, 168 Changhai Road, Shanghai 200433, China. Email  
address: [13601713431@163.com](mailto:13601713431@163.com).

Zhi-Fu Guo, Department of Cardiovascular Diseases, Changhai Hospital, Second Military Medical  
University, 168 Changhai Road, Shanghai 200433, China. Email address: [guozhifu@126.com](mailto:guozhifu@126.com)

The first two authors (MS, L-ZB) contributed equally to this work.

Short title: Obestatin's effect on aquaporin 2 membrane distribution

Funding: This work was supported by the National Natural Science Foundation of China  
(81470517).

Conflict of interest: The authors have no conflict of interest to declare.

## Abstract

**Background:** Previous studies have found that obestatin significantly inhibited water drinking and reduced the arginine vasopressin (AVP) levels in the brain to decrease renal water reabsorption. However, obestatin is unable to cross the blood–brain barrier. Its effect on the

body's kidney water metabolism in peripheral, remains unknown.

**Methods:** Expression and subcellular distribution of aquaporin 2 (AQP2) were detected by immunoblotting and immunofluorescence in mouse inner medullary collecting duct (mIMCD)-3 cells and congestive heart failure (CHF) model rats. Moreover, expression of the phosphorylation of AQP2(P-AQP2, Ser 256) in mIMCD-3 cells was evaluated by immunoblotting.

**Results:** After a 30-min treatment with obestatin in mIMCD-3 cells and CHF model rats, the AQP2 plasma membrane distribution decreased while corresponding protein level P-AQP2 (Ser256) level and phosphorylation ratio of AQP2 showed no significant change.

**Conclusions:** These findings suggest that obestatin has a short-term regulatory effect on the AQP2 plasma membrane distribution. In addition, obestatin decreases the AQP2 plasma membrane distribution probably by promoting the endocytosis of AQP2.

**Key words:** Obestatin; Aquaporin 2; Short-term regulation; Trafficking.

## Introduction

Obestatin, a 23-amino acid peptide derived from the same 117-residue prepropeptide as ghrelin, is mainly generated in the gastrointestinal tract tissue and is involved in body appetite and weight regulation.<sup>1</sup> Samson et al<sup>2,3</sup> have reported that intraventricular administration of

obestatin significantly inhibits water drinking in rats and reduces the arginine vasopressin (AVP) levels in a dose-dependent manner to decrease renal water reabsorption. In addition, it has been demonstrated that obestatin is unable to cross the blood–brain barrier via a saturable transport system.<sup>4-6</sup> Our previous study found that the concentration of plasma obestatin was significantly higher in patients with congestive heart failure (CHF), especially in those with cardiorenal syndrome, and was positively correlated with the AVP levels.<sup>7</sup> Therefore, we speculate that obestatin may regulate the body's water and electrolyte balance through AVP antagonization.

Aquaporin 2 (AQP2) is distributed in the plasma membrane and intracellular vesicles of principal cells in the kidney's collecting duct and connecting tubules.<sup>8</sup> It is a key protein that regulates the water permeability of the collecting duct, mainly participating in water reabsorption and urine enrichment to adjust electrolyte and fluid balance.<sup>9</sup> The distribution of AQP2 in the plasma membranes determines the ability of collecting duct principal cells to reabsorb water and then adjust the body's water balance. Any alteration of its distribution in the plasma membranes would induce both the body's water imbalance and corresponding disorders, including diabetes insipidus, the syndrome of inappropriate antidiuretic hormone secretion, hepatic cirrhosis, nephrotic syndrome, and chronic heart failure.<sup>10</sup>

The aim of this study was to investigate the short-term effect of obestatin on the localization of AQP2 and its possible mechanism.

## Methods

### Materials

Murine inner medullary collecting duct (mIMCD)-3 cells were purchased from JENNIO Biological Technology (Guangdong, China). Dulbecco's Modified Eagle Medium: Nutrient Mixture F-12 (DMEM/F-12), fetal calf serum (FBS), 0.25% trypsin-ethylenediaminetetraacetic acid (EDTA), and goat anti-rabbit immunoglobulin (Ig) G (H&L)-FITC were purchased from Thermo Fisher Corp. (Waltham, MA, USA). Desmopressin (dDavp) was purchased from Phoenix Biotech Co. Ltd. (San Antonio, TX, USA). Obestatin (OB) and nonamidated obestatin (NA-OB) were synthesized by GL Biochem Ltd. (Shanghai, China). Mozavaptan (OPC-31260; OPC) was purchased from Selleckchem Corp. (Houston, TX, USA). PhosSTOP phosphatase inhibitor cocktail was purchased from Roche Corp. (Basel, Switzerland). Anti-AQP2 antibody and anti-p-AQP2 (Ser256) antibody were purchased from Abcam Corp. (Cambridge, UK). Anti-GAPDH antibody and goat anti-rabbit IgG-HRP were purchased from Santa Cruz Biotechnology, Inc. (Dallas, TX, USA).

### Cell culture and intervention

Cells were cultured in complete medium (DMEM/F-12 supplemented with 10% FBS and 100u/ml penicillin-streptomycin) in a 5% CO<sub>2</sub> atmosphere at 37 °C. Cells were grown to confluence and cultured without FBS prior to stimulation. Then, the cells were treated with obestatin (100 nM and 1 μM), 100 nM NA-OB, 100 nM dDavp, and 100 nM OPC for 15 minutes, 30 minutes, and 60 minutes, separately. An equal volume of phosphate-buffered saline (PBS)

was used as a blank control.

#### Animal experiments

Pathogen-free male Sprague–Dawley rats (body weight 180~200 g) were provided by Shanghai SIPPR-BK Laboratory Animal Co. Ltd. [Animal license number: SCXK (Shanghai) 2013-0016]. The rats were fed commercial rat chow, given free access to water, and housed under a 12-hour light/12-hour dark cycle at a temperature of  $25 \pm 2^{\circ}\text{C}$ . All experimental protocols, which were in agreement with laboratory animal management and use regulations, had been approved by the Animal Care and Use Committee of Second Military Medical University before the performance of the study. All rats were acclimatized for 5 days before modeling. CHF was induced by myocardial infarction (MI) via ligation of the left anterior descending branch (LAD) of the coronary artery. Briefly, chloral hydrate 10% (350 mg/kg) was administered via intraperitoneal injection for anesthetization. Then, after sequential procedures of endotracheal intubation, ventilator-assisted breathing, depilation, operative skin region sterilization, thoracic opening, pericardium shearing, and exposure of the pulmonary cone, ligation of the bottom of the LAD about 2~3 mm away from the left atrial appendage was performed. For the rats assigned to the sham group, the same procedure was performed without ligation of the LAD. MI model rats were fed normally for 6 weeks. Then according to transthoracic echocardiography, the surviving rats were screened by the criterion of an ejection fraction (EF) value  $\leq 45\%$ <sup>11, 12</sup> as the successful CHF model. The selected CHF model rats were

randomly assigned to the following 3 groups ( $n = 6$  rats per group) according to different treatments: control group (physiological saline), obestatin group ( $100 \mu\text{g} / \text{kg BW}^{13}$ ) and OPC-31260 group ( $1 \text{ mg}/\text{rat}^{14}$ ). All reagents were given via the femoral vein to animals for 30 minutes, then kidneys were either immersion-fixed for immunofluorescence or removed for protein extraction.

#### Immunofluorescence

The mIMCD-3 cells were cultured on a 24-well plate containing coverslips and treated with different reagents, as described above. After the intervention, the cells on the coverslips were rinsed with phosphate-buffered saline (PBS) twice and then fixed with 4% paraformaldehyde at room temperature for 10 minutes. After washing with PBS 3 times for 5 minutes each, the cells were permeabilized with 0.1% Triton-X-100/PBS for 5 minutes, blocked with 5% goat serum for 30 minutes, and washed with PBS once. For immunofluorescence labeling, the cells on the coverslips were incubated with the primary antibody ( $1\mu\text{g}/\text{ml}$ ) at room temperature for 1 hour. Subsequently, the coverslips were rinsed with PBS 3 times for 5 minutes each and then reacted with goat anti-rabbit IgG (H&L)-FITC ( $2 \mu\text{g}/\text{ml}$ ) at room temperature for another hour. Finally, after washing 3 times with PBS, the nuclei were stained with DAPI ( $300 \text{ nM}$ ) for 2 minutes. The results were observed and imaged with a laser fluorescence confocal microscope.

Kidneys of rats were fixed in 4% neutral paraformaldehyde for 24 hours before dehydration with a gradient of ethanol concentrations. Dehydrated samples were embedded in

paraffin wax using a standard procedure, and then 5- $\mu$ m paraffin sections were prepared for immunofluorescence examination. Briefly, endogenous peroxidase was blocked in 3% H<sub>2</sub>O<sub>2</sub> for 10 minutes at room temperature. For antigen retrieval, sections were heated in a microwave oven and then boiled in a mixed retrieval solution (1 mM Tris, pH 9.9 with 0.5 mM EDTA) for 10 minutes. After cooling naturally, the sections were blocked in 5% goat serum for 30 minutes and washed with PBS once. Follow-up fluorescent labeling method was the same as mIMCD-3. The results were imaged with a fluorescence microscope. The fluorescence intensities of AQP2 in rat kidneys were quantified using Image-Pro plus Version 6.0 software.

#### Western blot analysis

Protein was extracted from approximately 50 mg renal inner medullary tissue or  $4 \times 10^5$  mIMCD-3 cells using RIPA lysis buffer with protease inhibitor (PMSF) and phosphatase inhibitor cocktail (AP, SP, PP1, PP2A, PP2B, PTP). The protein concentration was measured using the bicinchoninic acid protein assay method. Sample aliquots were mixed with sodium dodecyl sulfate (SDS) sample buffer, denatured in boiled water for 5 minutes, loaded on a 12% SDS-polyacrylamide gel, separated by electrophoresis, and transferred to polyvinylidene difluoride membranes. After blocking with 5% bovine serum albumin, the membranes were probed with the following primary antibodies: rabbit anti-AQP2 (1 $\mu$ g/ml), rabbit anti-p-AQP2 (Ser256, 1 $\mu$ g/ml), and rabbit anti-GAPDH (1 $\mu$ g/ml) at 4 °C overnight. After washing with tris-buffered saline–Tween 20 (TBST, pH 7.4) 3 times, the membranes were incubated with goat



anti-rabbit IgG-HRP (1ug/ml) for 2 hours at room temperature. Finally, the probed protein bands on the membranes were visualized using enhanced chemiluminescence after washing with TBST 3 times, and the ImageQuant LAS 4000 Gel Imaging System was used to capture the luminous protein bands. The target band intensities were quantified by Image J software, and the expression level was estimated by the ratio of the target band density/GAPDH band density.

#### Statistical analysis

All results were presented as means  $\pm$  standard error of the mean (mean  $\pm$  SD). SPSS 21.0 statistical software was used for the data analysis. The variance homogeneity test was performed by the Levene test. One-way analysis of variance was performed on the data, and the least significant difference t test was used to analyze the difference between the 2 groups. P values  $<0.05$  were accepted as statistically significant.

## Results

### Obestatin altered the subcellular distribution of AQP2 in mIMCD-3 cells

The plasma membrane distribution of AQP2 reflects the water balance-regulating ability of principle cells in the renal tubules.<sup>9</sup> To explore the effect of obestatin on AQP2, we treated mIMCD-3 cells with amidated obestatin (obestatin), which has been verified as an active form of obestatin,<sup>1</sup> or NA-OB at different time points, respectively. The subcellular distribution of AQP2 was then observed by immunofluorescence staining. No significant alteration of the AQP2 subcellular distribution was found after treatment with 100 nM obestatin for 15 minutes,

compared with pre-intervention. However, after a 30- or 60-minute treatment with 100 nM obestatin, the plasma membrane distribution of AQP2 was significantly decreased (Figure 1C). The pattern of AQP2 distribution on the plasma membrane after treatment with 1  $\mu$ M obestatin for the same time points was similar to those treated with 100 nM obestatin (Figure 1D). Interestingly, treatment with 100 nM NA-OB did not show any significant changes of AQP2 plasma membrane distribution at 15 minutes, 30 minutes, and 60 minutes, compared with pre-intervention (Figure 1B) which was completely similar to PBS (Figure 1A). AVP has been reported to be able to increase the AQP2 plasma membrane distribution, and low-dose OPC (such as 100 nM) is a selective antagonist of the AVP V2 receptor that downregulates the distribution of AQP2 in the plasma membrane.<sup>14, 15</sup> Thus, mIMCD-3 cells were treated with dDavp, an analog of AVP, and OPC as upregulated positive control group and downregulated positive control, separately. Clearly, after treatment with dDavp for 15 minutes, AQP2 slightly gathered in the plasma membrane compared with pre-intervention, and this plasma membrane distribution was obviously getting stronger after a 30-minute treatment. However, the increased plasma membrane distribution of AQP2 had disappeared after a 60-minute treatment, which did not show significant changes compared with pre-intervention (Figure 1E). There was no significant change of the distribution of AQP2 after treatment with OPC for 15 minutes compared with pre-intervention. However, after treatment with OPC for 30 or 60 minutes, the plasma membrane distribution of AQP2 was significantly decreased. (Figure 1F).

### AQP2 protein expression in mIMCD-3 cells after obestatin treatment

Continuously, the expression of AQP2 was detected by immunoblotting after the treatment described above. There was no significant difference in the AQP2 protein expression between each intervention group and the control group after a 15-minute treatment (Figure 2A). However, the AQP2 expression in the OPC-treated group was significantly decreased compared with the control group ( $P < 0.01$ ), after a 30-minute treatment. Meanwhile, the other groups did not show any significant difference ( $P > 0.05$ ) (Figure 2B). After a 60-minute treatment, the AQP2 expression in the groups treated with 100 nM obestatin (OB-L group), 1  $\mu$ M obestatin (OB-H group), 100 nM dDapv, or 100 nM OPC was significantly decreased, compared with the control group (all  $P < 0.01$ ). The NA-OB-treated group did not show any changes compared with the control group (Figure 2C).

### Phosphorylation of AQP2 (Ser256) in mIMCD-3 cells after obestatin stimulation

Next, we analyzed the phosphorylation of AQP2 in mIMCD-3 cells after obestatin stimulation because phosphorylation of AQP2 at serine 256 triggers AQP2 translocation from vesicles to the apical plasma membrane, which in turn increases water permeability of renal principal cells.<sup>16</sup> The P-AQP2 level clearly increased after dDapv stimulation for 15 minutes ( $P < 0.01$ ), whereas the P-AQP2 level did not show any difference in the other groups, compared with the control group (Figure 3A). Compared with the control group after a 30-minute stimulation, the P-AQP2 level in the OPC group was significantly decreased ( $P < 0.01$ ); however,

no significant changes were observed in the other groups (Figure 3B). Notably, the P-AQP2 level in the OB-L group, OB-H group, and OPC group was significantly reduced after a 60-minute stimulation, compared with that in the control group (all  $P < 0.01$ ); meanwhile, no significant changes were found in either the NA-OB or dDAVP group compared with the control (Figure 3C).

To compare the phosphorylation levels of AQP2 (Ser256) better, we calculated the ratio of P-AQP2 to total AQP2. Compared with the control group, the phosphorylation ratio of AQP2 in dDAVP group was significantly increased after a 15-minute treatment ( $P < 0.01$ ) and there was no significant change shown in the other groups (Figure 4A). After a 30-minute treatment, the phosphorylation ratio of AQP2 in OPC group was significantly decreased compared to the control group ( $P < 0.05$ ) and no significant change was observed in the other groups (Figure 4B). After a 60-minute treatment, the phosphorylation ratio of AQP2 in dDAVP group was significantly higher than that in the control group ( $P < 0.05$ ) and no significant change was shown in the other groups (Figure 4C).

Short-Term effects of obestatin on AQP2 subcellular distribution and protein expression in renal inner medullary tissue

To confirm the short-term regulatory effect of obestatin on AQP2 traffic *in vivo*, the CHF rats were treated with obestatin for 30 minutes while the CHF model rats treated with OPC as positive control and physiological saline as control group. The immunofluorescent analysis of renal inner medullary collecting ducts showed that AQP2 accumulated at the plasma membrane

in the control group, while AQP2 was evenly distributed at the plasma membrane and intracellular vesicles in the obestatin group (Figure 5A). However, the AQP2 protein expression showed no significant change between the obestatin group and control (Figure 5B). Clearly, both the plasma membrane distribution of and the protein expression of AQP2 in OPC group was significantly decreased compared with the control group as expected (Figure 5).

## Discussion

The change of subcellular distribution of AQP2 is known as the trafficking or short-term regulation of AQP2.<sup>15,17</sup> There exists a dynamic equilibrium between the exocytic insertion of AQP2 into the apical plasma membrane and the endocytic removal of AQP2 from the apical plasma membrane. In our observations, the distribution of AQP2 in plasma membrane of mIMCD-3 cells and renal inner medullary tissue was decreased after treatment with obestatin for 30 minutes by immunofluorescence staining (Figure 1C, Figure 1D and Figure 5A). Additionally, AQP2 protein expression showed no change after obestatin treatment for 30 minutes (Figure 2B and Figure 5B). These findings indicate that obestatin has a regulatory effect on AQP2 trafficking, which is known as the short-term regulation of AQP2.<sup>10</sup> In other words, obestatin can downregulate the plasma membrane distribution of AQP2 through short-term regulation. On the other hand, NA-OB, the nonamidated form of obestatin, did not show any of this modulating ability, which verified again that the active form of obestatin is amidated obestatin; this finding is consistent with the view that NA-OB has low activity as described by

Zhang *et al.*<sup>1</sup>

The short-term regulation of AQP2 is controlled through the sustained processes of exocytosis and endocytosis.<sup>18</sup> Downregulation of AQP2 in the plasma membrane can be achieved by prohibiting the exocytosis of AQP2 or promoting the endocytosis of AQP2. S256 phosphorylation of AQP2 is the essential and critical process for its accumulation in the apical membrane of collecting duct principal cells by exocytosis.<sup>19</sup> The P-AQP2 (Ser256) level in mIMCD-3 cells was detected to explore whether Ser256 phosphorylation/dephosphorylation was involved in the mechanism by which obestatin regulates the AQP2 subcellular distribution.

Our findings indicated that both AQP2 protein expression and the P-AQP2 (S256) level did not change after a 15- or 30-minute treatment with obestatin (Figures 2 and 3), while the distribution of AQP2 in the mIMCD-3 cellular plasma membrane was decreased at the 30-minute time point (Figures 1C and D). And the phosphorylation ratio of AQP2 (Ser256) showed no change after treatment with obestatin (Figure 4). It indicates that Ser256 phosphorylation/dephosphorylation is not involved in the regulatory effect of obestatin on AQP2 distribution, which means that obestatin downregulates AQP2 plasma membrane distribution probably by promoting the endocytosis of AQP2. Furthermore, increased endocytosis may further lead to the degradation of AQP2,<sup>20</sup> leading to a decrease of AQP2 protein expression levels (Figure 2C). The decrease of P-AQP2 (S256) level at the 60-minute time point may be due to the decrease of AQP2 protein expression levels (Figure 3C). However, the details and specific mechanisms need to be further studied.

Our results showed that the P-AQP2 (Ser256) level increased after a 15-minute treatment with dDavp (Figure 3A), while the plasma membrane distribution of AQP2 was not changed in mIMCD-3 cells (Figure 1E). However, after a 30-minute treatment with dDavp, the plasma membrane distribution of AQP2 increased (Figure 1E) and the P-AQP2 level reduced to normal. These results indicate that regulation of the AQP2 plasma membrane distribution through AVP is a quick process, which is consistent with the above-mentioned AVP-regulated mechanism. However, there was a flaw in this part of the results that the ruffling effect of AVP may affect the graph captured. The AQP2 expression decreased after a 60-minute treatment with dDavp (Figure 2C), contradicting the upregulatory effect of AVP on AQP2 expression. The reason may be that dDavp stimulates AQP2 decomposition in a short time,<sup>21</sup> which also explained the reason that the phosphorylation ratio of AQP2(Ser256) increased after treatment with dDavp for 60 minutes (Figure 4C).

AQP2 plays an important role in maintaining the body's water balance. An increased distribution of AQP2 in the apical plasma membrane of the kidney's collecting duct cells triggers water intake to cause water retention, which is believed to be one of the vital pathophysiological mechanisms for congestive heart failure.<sup>22</sup> The development of new diuretics focusing on the AQP2 regulatory pathway is the major direction for current heart failure treatment; for example, tolvaptan, a V2 receptor antagonist, has been successfully applied clinically.<sup>23</sup> Our results that obestatin downregulates the AQP2 distribution in the plasma membrane, combined with our previous finding that obestatin increases the circulation

in patients with heart failure, confirmed that obestatin can antagonize AVP through downregulation of the AQP2 apical membrane distribution to reduce water reabsorption, increase urine volume, and then decrease water retention. This mechanism may reflect the body's internal control of the water balance in congestive heart failure. However, we have to note that the experiments were conducted in cell cultures not fully confluent and using a hypo osmotic fixative solution. These two conditions could have affected the results of our experiments. Also, further experiments will be needed to determine the role of obestatin in other areas of the kidney (e.g, cortex). This mechanism needs to be supported by further experiments, which may create a method to develop new diuretics for heart failure treatment.

### Author Contributions

M.S. and L-Z.B. carried out the experiment. M.S. wrote the manuscript with support from X.Z. and X-X.Z. Z-F.G. conceived the original idea. X-X.Z. and Z-F.G helped supervise the project.

### References

1. Zhang JV, Ren PG, Avsian-Kretchmer O, et al. Obestatin, a peptide encoded by the ghrelin gene, opposes ghrelin's effects on food intake *Science* 2005;310:996-9.
2. Samson WK, White MM, Price C, et al. Obestatin acts in brain to inhibit thirst *Am J Physiol Regul Integr Comp Physiol* 2007;292:R637-43.
3. Samson WK, Yosten GL, Chang JK, et al. Obestatin inhibits vasopressin secretion: evidence for a physiological action in the control of fluid homeostasis *J Endocrinol* 2008;196:559-64.
4. Pan W, Tu H, Kastin AJ. Differential BBB interactions of three ingestive peptides: obestatin, ghrelin, and adiponectin *Peptides* 2006;27:911-6.
5. Zizzari P, Longchamps R, Epelbaum J, et al. Obestatin partially affects ghrelin stimulation of



- food intake and growth hormone secretion in rodents *Endocrinology* 2007;148:1648-53.
6. Vergote V, Van Dorpe S, Peremans K, et al. In vitro metabolic stability of obestatin: kinetics and identification of cleavage products *Peptides* 2008;29:1740-8.
  7. Shi JB, Guo ZF, Zheng X, et al. Circulating obestatin is increased in patients with cardiorenal syndrome and positively correlated with vasopressin *Peptides* 2012;38:377-80.
  8. Takata K, Matsuzaki T, Tajika Y, et al. Localization and trafficking of aquaporin 2 in the kidney *Histochem Cell Biol* 2008;130:197-209.
  9. Nielsen S, Frokiaer J, Marples D, et al. Aquaporins in the kidney: from molecules to medicine *Physiol Rev* 2002;82:205-44.
  10. Wilson JL, Miranda CA, Knepper MA. Vasopressin and the regulation of aquaporin-2 *Clin Exp Nephrol* 2013;17:751-64.
  11. Zhang L, Gan ZK, Han LN, et al. Protective effect of heme oxygenase-1 on Wistar rats with heart failure through the inhibition of inflammation and amelioration of intestinal microcirculation *J Geriatr Cardiol* 2015;12:353-65.
  12. Wang XF, Qu XQ, Zhang TT, et al. Testosterone suppresses ventricular remodeling and improves left ventricular function in rats following myocardial infarction *Exp Ther Med* 2015;9:1283-91.
  13. Koc M, Kumral ZN, Ozkan N, et al. Obestatin improves ischemia/reperfusion-induced renal injury in rats via its antioxidant and anti-apoptotic effects: role of the nitric oxide *Peptides* 2014;60:23-31.
  14. Christensen BM, Marples D, Jensen UB, et al. Acute effects of vasopressin V2-receptor antagonist on kidney AQP2 expression and subcellular distribution *Am J Physiol* 1998;275:F285-97.
  15. Nielsen S, Chou CL, Marples D, et al. Vasopressin increases water permeability of kidney collecting duct by inducing translocation of aquaporin-CD water channels to plasma membrane *Proc Natl Acad Sci U S A* 1995;92:1013-7.
  16. Balasubramanian L, Sham JS, Yip KP. Calcium signaling in vasopressin-induced aquaporin-2 trafficking *Pflugers Arch* 2008;456:747-54.
  17. Moeller HB, Praetorius J, Rutzler MR, et al. Phosphorylation of aquaporin-2 regulates its endocytosis and protein-protein interactions *Proc Natl Acad Sci U S A* 2010;107:424-9.
  18. Noda Y. Dynamic regulation and dysregulation of the water channel aquaporin-2: a common cause of and promising therapeutic target for water balance disorders *Clin Exp Nephrol* 2014;18:558-70.
  19. Arnspang EC, Login FH, Koffman JS, et al. AQP2 Plasma Membrane Diffusion Is Altered by the Degree of AQP2-S256 Phosphorylation *Int J Mol Sci* 2016;17.
  20. Vukicevic T, Schulz M, Faust D, et al. The Trafficking of the Water Channel Aquaporin-2 in Renal Principal Cells-a Potential Target for Pharmacological Intervention in Cardiovascular Diseases *Front Pharmacol* 2016;7:23.
  21. Hasler U, Mordasini D, Bens M, et al. Long term regulation of aquaporin-2 expression in

vasopressin-responsive renal collecting duct principal cells J Biol Chem 2002;277:10379-86.

22. Ziaeian B, Fonarow GC. Epidemiology and aetiology of heart failure Nat Rev Cardiol 2016;13:368-78.

23. Izumi Y, Miura K, Iwao H. Therapeutic Potential of Vasopressin-Receptor Antagonists in Heart Failure Journal of Pharmacological Sciences 2014;124:1-6.

ACCEPTED MANUSCRIPT

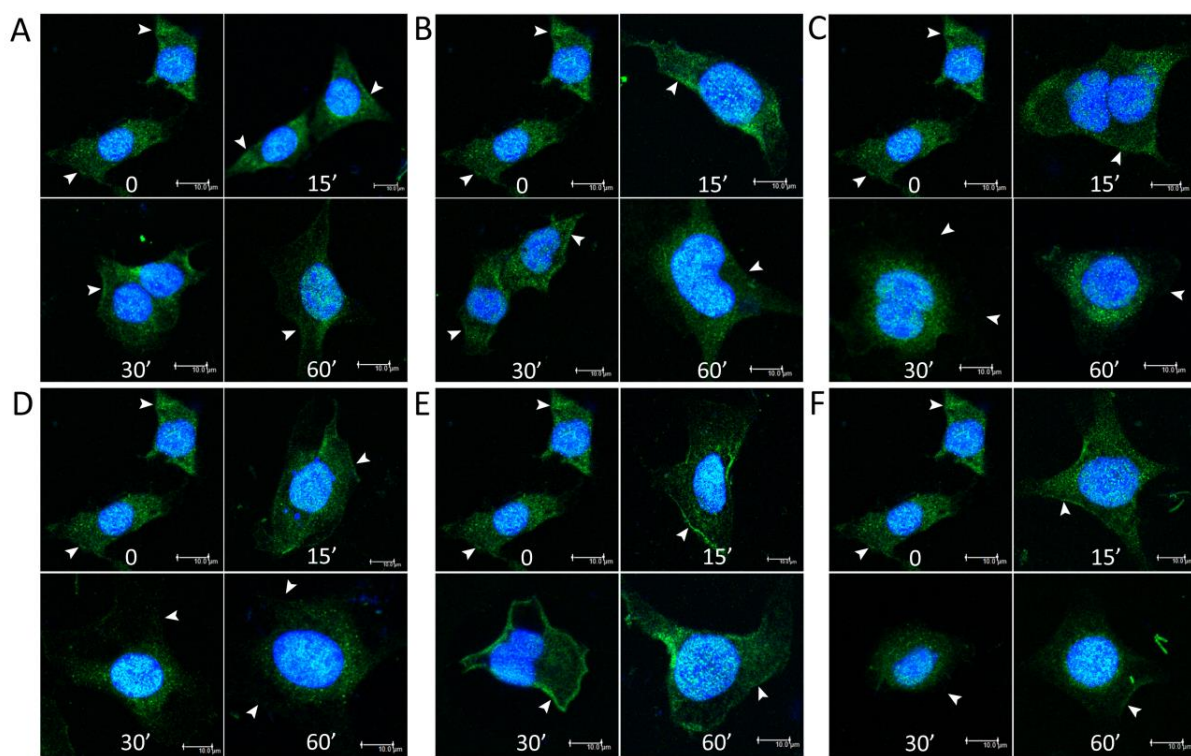


**Figure 1.** Obestatin decreased the plasma membrane distribution of AQP2 in mIMCD-3 cells. mIMCD-3 cells were pretreated with PBS (A), 100 nM NA-obestatin (B), 100 nM obestatin (C), 1  $\mu$ M obestatin (D), 100 nM dDapv (E), and 100 nM OPC-31260 (F) for 0 (a), 15 (b), 30 (c), and 60 (d) minutes, respectively. AQP2 (green) was stained with rabbit anti-AQP2 antibody. Nuclei were stained with DAPI (blue). Membrane was labeled with arrowheads. Representative confocal images of 3 independent experiments are shown. Scale bars, 10  $\mu$ m. Abbreviations: AQP2, aquaporin 2; mIMCD-3, mouse inner medullary collecting duct; PBS, phosphate-buffered saline.

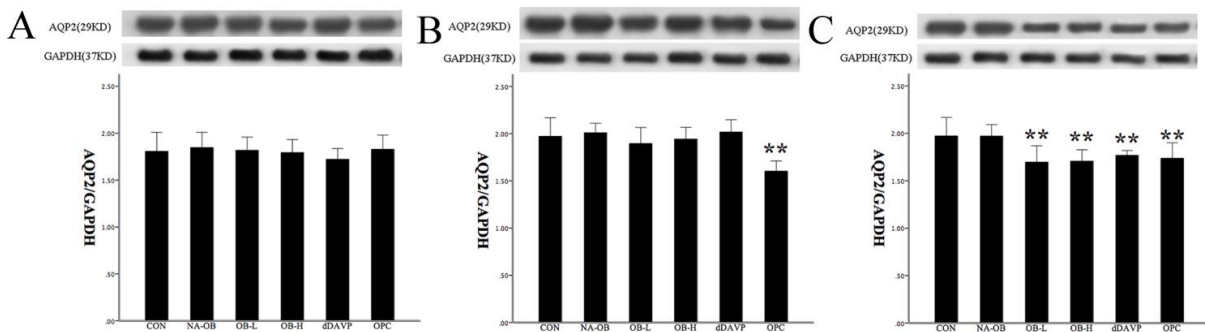


**Figure 2.** AQP2 protein expression in mIMCD-3 cells after obestatin stimulation. mIMCD-3 cells were stimulated with PBS (CON), 100 nM NA-obestatin (NA-OB), 100 nM obestatin (OB-L), 1  $\mu$ M obestatin (OB-H), 100 nM dDAvp (dDAvp), and 100 nM OPC-31260 (OPC) for 15 (A), 30 (B), and 60 (C) minutes, respectively. The AQP2 protein expression was evaluated by western blot using the rabbit anti-AQP2 antibody. Representative blots of 3 independent experiments are shown. Error bars are mean values  $\pm$  SD from 3 experiments. Abbreviations: AQP2, aquaporin 2; mIMCD-3, mouse inner medullary collecting duct cells; PBS, phosphate-buffered saline; SD, standard deviation.

\*\*  $P < 0.01$ , compared with the control.

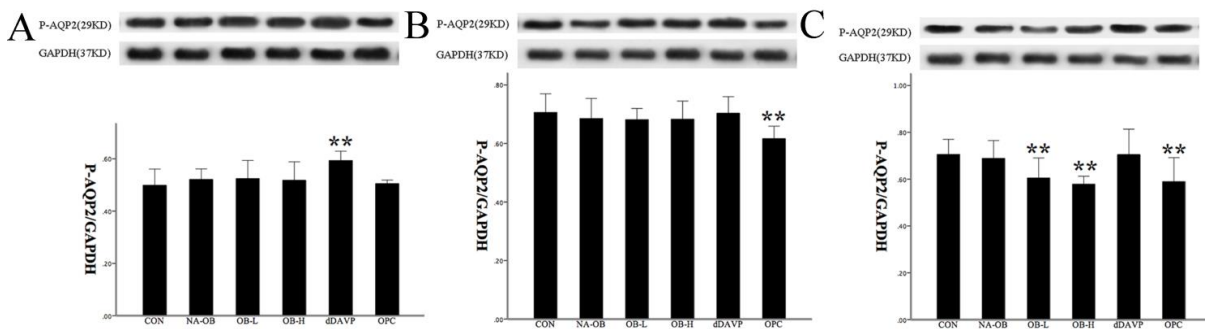


**Figure 3.** Phosphorylation of AQP2 (Ser256) (P-AQP2) in mIMCD-3 cells after obestatin stimulation. mIMCD-3 cells were stimulated with PBS (CON), 100 nM NA-obestatin (NA-OB), 100 nM obestatin (OB-L), 1  $\mu$ M obestatin (OB-H), 100 nM dDAVP (dDAVP), and 100 nM OPC-31260 (OPC) for 15 (A), 30 (B), and 60 (C) minutes, respectively. Phosphorylation of AQP2 (Ser256) (P-AQP2) was analyzed by western blot by rabbit anti-p-AQP2 antibody. Representative blots of 3 independent experiments are shown. Error bars are mean values  $\pm$  SD from 3 experiments. Abbreviations: AQP2, aquaporin 2; mIMCD-3, mouse inner medullary collecting duct cells; PBS, phosphate-buffered saline; SD, standard deviation.

\*\*  $P < 0.01$ , compared with the control.

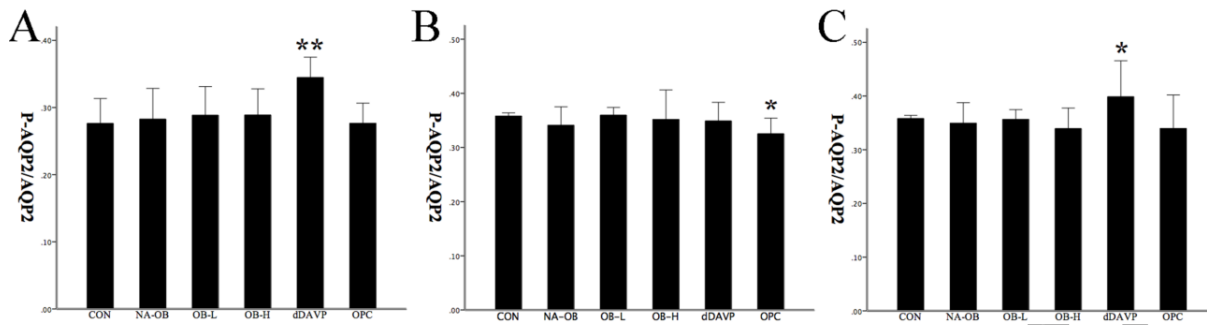


**Figure 4.** Changes of phosphorylation ratio of AQP2 (Ser256) by different interventions. The ratio of P-AQP2 (Ser256) to total AQP2 was calculated after the mIMCD-3 cells been stimulated with PBS (CON), 100 nM NA-obestatin (NA-OB), 100 nM obestatin (OB-L), 1  $\mu$ M obestatin (OB-H), 100 nM dDAVP (dDAVP), and 100 nM OPC-31260 (OPC) for 15 (A), 30 (B), and 60 (C) minutes, respectively. Error bars are mean values  $\pm$  SD from 3 experiments. Abbreviations: AQP2, aquaporin 2; mIMCD-3, mouse inner medullary collecting duct cells; PBS, phosphate-buffered saline; SD, standard deviation.

\*  $P < 0.05$ , compared with controls.

\*\*  $P < 0.01$ , compared with controls.

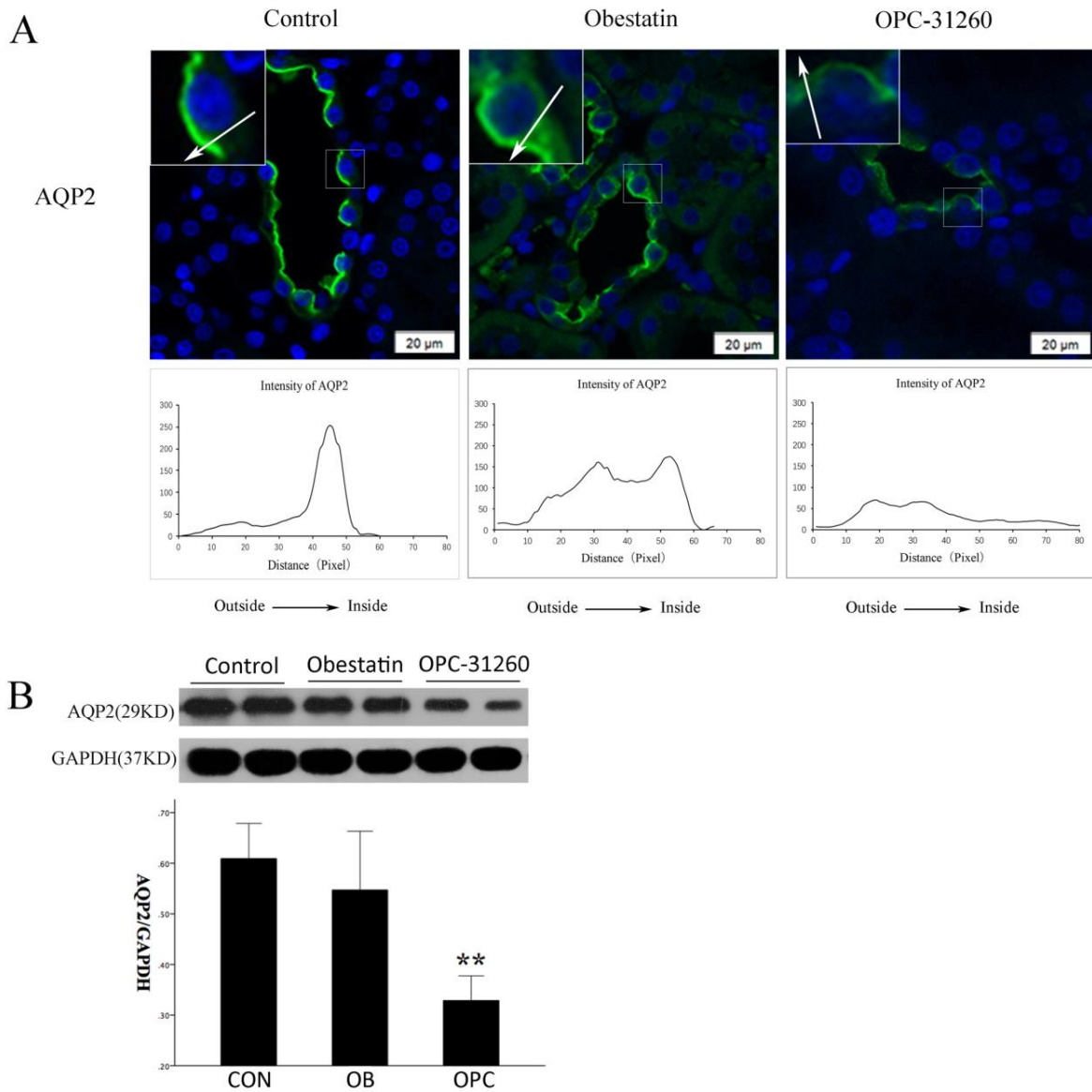


**Figure 5.** Short-term effects of obestatin on AQP2 subcellular distribution and protein expression in renal inner medullary tissue. CHF model rats were Intravenously injected with obestatin (100  $\mu$ g /kg BW), OPC-31260(1 mg/rat) or physiological saline for 30 minutes. (A) Immunofluorescence staining of AQP2 in renal inner medullary tissue. AQP2 (green) was stained

with rabbit anti-AQP2 antibody. Nuclei were stained with DAPI (blue). Representative collecting duct cells are enlarged in the inset at top left. Representative immunofluorescence images of 6 independent experiments are shown. Scale bars, 20  $\mu\text{m}$ . The relative intensities of AQP2 staining from outer to apical membrane (along the arrow) were shown. (B) Western blot analysis of AQP2 in rat renal inner medullary tissue. The AQP2 protein expression was evaluated by western blot using the rabbit anti-AQP2 antibody. Representative blots of 3 independent experiments are shown. Error bars are mean values  $\pm$  SD from 3 experiments. Abbreviations: AQP2, aquaporin 2; CHF, congestive heart failure; SD, standard deviation.

\*\*  $P < 0.01$ , compared with the control.

ACCEPTED MANUSCRIPT